Hindawi
International Journal of Aerospace Engineering
Volume 2021, Article ID 9269438, 10 pages
https://doi.org/10.1155/2021/9269438

Research Article

Neural Network-Based Finite-Time Fault-Tolerant Control for Spacecraft without Unwinding

Chao Tan,[1] Guodong Xu,[1] Limin Dong,[1] Han Zhao,[2] Jun Li,[3] and Sai Zhang[2]

[1]*School of Astronautics, Harbin Institute of Technology, Harbin 150001, China*
[2]*College of Aerospace and Civil Engineering, Harbin Engineering University, Harbin 150001, China*
[3]*School of Automation, Harbin Engineering University, Harbin 150001, China*

Correspondence should be addressed to Jun Li; lijun1221@hrbeu.edu.cn

Received 2 February 2020; Revised 29 December 2020; Accepted 15 February 2021; Published 24 February 2021

Academic Editor: Yue Wang

In this paper, we focus on solving the problems of inertia-free attitude tracking control for spacecraft subject to external disturbance, unknown inertial parameters, and actuator faults. The robust control architecture is designed by using the rotation matrix and neural networks. In the presence of external disturbance and parametric uncertainties, a fault-tolerant control (FTC) scheme synthesized with the minimum-learning-parameter (MLP) algorithm is proposed to improve the reliability of the system when unknown actuator faults occur. These methods are developed based on backstepping to ensure that finite-time convergence is achievable for the entire closed-loop system states with low computational complexity. The validity and advantage of the designed controllers are highlighted by using Lyapunov-based analysis. Finally, the simulation results demonstrate the satisfactory performance of the developed controllers.

1. Introduction

With the rapid development of space engineering, spacecraft attitude control has been studied extensively by researchers for its essential role in various space missions, involving deep space exploration, earth observation, Mars detection, etc. As an important part of spacecraft, control systems determine the success of these missions for the most part. However, designing controllers with satisfactory performance for spacecraft still remains a challenging task, which can be attributed to complex external disturbance, unknown inertial parameters, and actuator faults. Despite these obstacles, numerous methods have been designed to address the attitude tracking control problem, including backstepping control [1–4], sliding mode control [5–7], prescribed performance control [8–10], and event-triggered control [11, 12].

Though fruitful results have been obtained for attitude control of spacecraft during the last decades, it still remains a challenge to design finite-time controllers under the circumstances of the external disturbance and unknown inertial matrix. On the one hand, modern space missions put forward high requirements in fast response and strong robustness for attitude control systems, which could be resorted to finite-time control strategies [13, 14]. On the other hand, inertial parameters are always time-varying with continuing fuel consumption during space missions, which makes it challenging to acquire accurate values of the inertial matrix. On account of the fast response requirement, finite-time control strategies [15–18] and appointed time approaches [19, 20] were adopted in the spacecraft system such that the control objective could be accomplished within a limited time. In [17, 18], terminal sliding mode-based methods were proposed for a single spacecraft and multiple spacecraft, respectively. Different from these two controllers, the prescribed performance control strategy was adopted in [19, 20], where the convergence time of the spacecraft system could be predefined by utilizing a nonlinear function. As for the unknown system parameters, NN-based control schemes [21, 22] were widely adopted for nonlinear systems, which have also been used to approximate unknown system dynamics in spacecraft systems [23, 24]. As for the stabilization of fractional-order systems with unknown parameters, the T-S fuzzy control theory synthesized with adaptive linear-like control rules shows its superior capability in dealing with uncertainties [25].

Apart from the fast response and unknown system parameters, actuator faults are another important aspect that deserves special attention, especially for the need for high reliability in space activities, such as rendezvous and docking. Complex space environments and disturbances render the spacecraft vulnerable to actuator faults, which will deteriorate the control performance. To address this issue, researchers have introduced FTC schemes for various space applications [26–28]. Niu et al. proposed an observer-based FTC strategy for attitude stabilization of rigid spacecraft when time-varying faults occur [27]. Aiming at attitude synchronization control for multiple spacecraft, Zhou and Xia introduced a fault-tolerant method in the presence of modeling uncertainties [28]. With much more superiority in nonlinear fractional-order systems, Hashtarkhani and Khosrowjerdi proposed a fault-tolerant controller in conjunction with the backstepping terminal sliding mode technique for an uncertain faulty system [29]. Besides, fractional adaptive state feedback control laws based on backstepping were developed in [30] to help promote the stability of the system with actuator failures.

Obviously, controllers in [26–28] have been constructed by using unit quaternion-based attitude descriptions, which have the inherent disadvantage of the unwinding problem. Due to this drawback, researchers focused on the rotation matrix-based attitude description, which can represent attitude motions globally and uniquely [31–33]. By resorting to the rotation matrix, Huang et al. proposed a fault-tolerant attitude tracking controller with finite-time stability [33]. Similarly, several control algorithms have been designed for rigid spacecraft with consideration of the unwinding problem [31, 32]. However, these controllers are not applicable for cases that inertial parameters are unknown. Therefore, further research is required to deal with the actuator fault, unknown system parameters, and unwinding problem.

Inspired by the aforementioned obstacles in controller design for spacecraft, this paper focuses on providing two unwinding-free attitude tracking control architectures for spacecraft when there exist actuator faults and unknown inertial parameters. The main contributions of this paper are given as follows:

(i) A finite-time attitude tracking controller is constructed on the basis of the rotation matrix with unknown inertial parameters, so that finite-time tracking performance could be obtained for spacecraft attitude control. Compared with existing methods [16, 33], inertial parameters could remain unavailable, making the tracking controllers more applicable in aerospace engineering

(ii) Actuator faults and unknown system dynamics could be handled simultaneously with the aid of the FTC strategy proposed in this paper. Based on the MLP algorithm, unknown system dynamics can be approximated with low computational complexity

The rest of this paper is organized as follows. In Section 2, the spacecraft model and preliminaries are presented. In Section 3, backstepping controllers are designed by utilizing MLP and FTC. In Section 4, the effectiveness of the proposed algorithms is validated through numerical simulations. Finally, the conclusions of this paper are presented in Section 5.

2. Spacecraft Model and Preliminaries

2.1. Spacecraft Attitude Dynamics. The unit quaternion has been widely used for attitude description in most attitude controllers [9–11]. However, the unit quaternion-based algorithm results in the unwinding problem with high fuel consumption. To address this problem, the rotation matrix is adopted here to describe the attitude dynamics of the spacecraft, which can be defined as follows:

$$\dot{R} = R\omega^{\times}, \tag{1}$$

$$J\dot{\omega} = -\omega^{\times} J\omega + \delta u + d, \tag{2}$$

where $R \in SO(3)$ denotes the rotation matrix; $\omega \in R^{3\times1}$ is the angular velocity; $J \in R^{3\times3}$ denotes the inertial matrix; $u \in R^{3\times1}$ and $d \in R^{3\times1}$ are the control torque and external disturbance of the spacecraft, respectively; and $\delta = \text{diag}\,(\delta_1, \delta_2, \delta_3)$ is the fault coefficient, where $0 < \theta < \delta_i \leq 1$, $i = 1, 2, 3$, with θ being a positive constant. For a vector $a = [a_1, a_2, a_3]^T$, $a^{\times}$ is defined as follows:

$$a^{\times} = \begin{bmatrix} 0 & -a_3 & a_2 \\ a_3 & 0 & -a_1 \\ -a_2 & a_1 & 0 \end{bmatrix}. \tag{3}$$

For the attitude controller design, attitude and angular velocity tracking errors $\tilde{R}$ and $\tilde{\omega}$ are defined in Equations (4) and (5), respectively, where $R_d \in SO(3)$ and $\omega_d \in R^{3\times1}$ are the commanded rotation matrix and angular velocity, respectively.

$$\tilde{R} = R_d^T R, \tag{4}$$

$$\tilde{\omega} = \omega - \tilde{R}^T \omega_d. \tag{5}$$

Thus, the attitude dynamics can be rewritten as follows:

$$\dot{\tilde{R}} = \tilde{R}\tilde{\omega}^{\times}, \tag{6}$$

$$J\dot{\tilde{\omega}} = F + \delta u + d, \tag{7}$$

where $F = -(\tilde{\omega} + \tilde{R}^T \omega_d)^{\times} J(\tilde{\omega} + \tilde{R}^T \omega_d) - J\tilde{R}^T \dot{\omega}_d + J\tilde{\omega}^{\times}\tilde{R}^T \omega_d$.

Attitude error functions presented in Equations (8) and (9) were selected to facilitate the attitude controller design.

$$e_{\tilde{R}} = \frac{1}{2\sqrt{1+\operatorname{tr}(\tilde{R})}}\left(\tilde{R}-\tilde{R}^T\right)^{\vee}, \tag{8}$$

$$\psi(\tilde{R}) = 2-\sqrt{1+\operatorname{tr}(\tilde{R})}. \tag{9}$$

Here, $\vee$ denotes the inverse operation of $\times$. Combining Equations (1)–(9), error dynamics can be reconstructed as follows:

$$\dot{e}_{\tilde{R}} = E\tilde{\omega}, \tag{10}$$

$$J\dot{\tilde{\omega}} = F + \delta u + d, \tag{11}$$

$$E = \frac{1}{2\sqrt{1+\operatorname{tr}(\tilde{R})}}\left(\operatorname{tr}(\tilde{R})I-\tilde{R}^T+2e_{\tilde{R}}e_{\tilde{R}}^T\right), \tag{12}$$

$$F = -\left(\tilde{\omega}+\tilde{R}^T\omega_d\right)^{\times}J\left(\tilde{\omega}+\tilde{R}^T\omega_d\right)-J\tilde{R}^T\dot{\omega}_d+J\tilde{\omega}^{\times}\tilde{R}^T\omega_d. \tag{13}$$

Remark 1. To ensure Equation (10) is valid, $\operatorname{tr}(\tilde{R}) \neq -1$ must be satisfied. As stated by Huang et al., $\operatorname{tr}(\tilde{R}) \neq -1$ can be derived if the condition $\|e_{\tilde{R}}\| \le 1$ is true [31–33]. Consequently, $\|e_{\tilde{R}}\| \le 1$ must be satisfied during space missions.

Remark 2. The inertial parameters J are regarded as unknown variables in the controller design. Minimum-learning-parameter algorithm-based NNs are employed to manage the unknown inertial matrix. In order to facilitate the controller design, the inertial matrix J is assumed to be a positive definite diagonal matrix.

2.2. Assumptions. The following assumption is necessary for the attitude controller design:

Assumption 1. The external disturbance d and commanded angular velocity ω_d are bounded and satisfy $\|d\| \le D$ and $\|\dot{\omega}_d\| \le \bar{\omega}$, where D and $\bar{\omega}$ are positive constants.

2.3. Mathematical Notation. In this paper, the notation $\|\cdot\|$ denotes the Euclidean norm of a vector or the induced norm of a matrix. For any $\xi \in R$, $\operatorname{sig}(\xi)^{\chi}$ is defined as $\operatorname{sig}(\xi)^{\chi} = [\operatorname{sign}(\xi)|\xi|^{\chi}]$. For a vector $\xi = [\xi_1, \xi_2, \cdots, \xi_n]^T$, $\operatorname{sig}(\xi)^{\chi}$ is defined as $\operatorname{sig}(\xi)^{\chi} = [\operatorname{sign}(\xi_1)|\xi_1|^{\chi}, \cdots, \operatorname{sign}(\xi_n)|\xi_n|^{\chi}]^T$. Here, χ is a constant that satisfies $0 < \chi < 1$. Furthermore, $\tanh(\xi) = [\tanh(\xi_1), \tanh(\xi_2), \cdots, \tanh(\xi_n)]^T$. For a matrix A, the notation $\lambda_{\max(A)}$ and $\lambda_{\min(A)}$ represent the maximum eigenvalue and minimum eigenvalue of A, respectively.

2.4. Related Lemmas. For the satisfactory performance in approximating functions, RBF NNs have been widely used in controller design for nonlinear systems. Therefore, RBF NNs are employed herein to address the unknown system dynamics caused by the unavailable inertial matrix. The following lemmas are introduced to facilitate the design process.

Lemma 3 [20]. *For a random continuous function $f(x)$, an ideal weight vector W exists that satisfies the following function:*

$$f(x) = W^T h(x) + \varepsilon, \tag{14}$$

where $W = [w_1, w_2, \cdots, w_p]^T$ and $x = [x_1, x_2, \cdots, x_m]$ are Ge-Lee vectors defining weight and input vectors, respectively; p and m are the node and input number, respectively; ε is the approximation error; and $h(x) = [h_1(x), \cdots, h_2(x)]^T$ is the Gaussian basis function vector with the following form:

$$h_i(x) = \exp\left(-\frac{\|x-c_i\|_2^2}{2b_i^2}\right), \quad i = 1, \cdots, p, \tag{15}$$

where $c_i \in R^m$ and $b_i \in R$ are the center vector and Gaussian basis function vector of $h_i(x)$, respectively.

Lemma 4 [33]. *If a vector $x \in R^3$ satisfies $R_d^T R = \exp(x^{\times})$, the inequality is always tenable. The term E defined in Equation (12) satisfies $\|E\| = 1/2$. Additionally, if $\|x\| \neq \pi$, E is always invertible.*

Lemma 5 [33]. *Considering positive constants ρ and α_i, $i = 1, 2, \cdots, n$, if the inequality $1 < \rho < 2$ holds, the following equation is obtained:*

$$\left(\alpha_1^2+\cdots+\alpha_n^2\right)^{\rho} \le \left(\alpha_1^{\rho}+\cdots+\alpha_n^{\rho}\right)^2. \tag{16}$$

Lemma 6 [33]. *For the system Equations (19) and (20), if a Lyapunov function V_1 exists such that it satisfies the following equation:*

$$\dot{V}_1 \le -aV_1^{\alpha}, \tag{17}$$

where a and α are positive constants satisfying $0 < \alpha < 1$, then the system converges to the origin within a finite time.

Lemma 7 [34, 35]. *Given positive scalers $x \in R$ and $\sigma > 0$, the following key inequation can be derived:*

$$0 \le |x| - \frac{|x|^2}{\sqrt{x^2+\sigma^2}} \le |x| - \frac{|x|^2}{|x|+\sigma} < \sigma. \tag{18}$$

3. Design of the Controller

In this section, a fault-tolerant attitude tracking controller is presented to ensure the stability of the closed-loop system with finite-time convergence. For better applicability, MLP and adaptive laws are proposed to estimate unknown system information. Besides, a backstepping-based FTC scheme is proposed with an auxiliary system, thus improving system reliability when an unknown actuator fault occurs.

Previous to designing the attitude controller, it is necessary to define $x_1 = e_{\tilde{R}} = [x_{11}, x_{12}, x_{13}]^T$ and $x_2 = E\tilde{\omega} - \tilde{\omega}_{p,1} = [x_{21}, x_{22}, x_{23}]^T$, so that the error dynamics in Equations (10) and (11) can be expressed as follows:

$$\dot{x}_1 = E\tilde{\omega}, \tag{19}$$

$$\dot{x}_2 = \dot{E}\tilde{\omega} + EJ^{-1}(F + \delta u + d) - \dot{\tilde{\omega}}_{p,1}. \tag{20}$$

Step 1. To prove that x_1 converges to a region containing the origin within a finite time, the virtual angular velocity $\tilde{\omega}_{p,1}$ is expressed as follows:

$$\tilde{\omega}_{p,1} = -k_1 \frac{x_1}{\sqrt{\|x_1\|^2 + \sigma^2}} - k_2 x_1, \tag{21}$$

where k_1 and k_2 are positive constants and k_2 should satisfy $k_2 > 1/2$.

The Lyapunov function is defined as follows:

$$V_1 = \frac{1}{2} x_1^T x_1. \tag{22}$$

By the utilization of Equations (19)–(21) as well as $x_2 = E\tilde{\omega} - \tilde{\omega}_{p,1}$, the derivative of V_1 can be derived as follows:

$$\begin{aligned} \dot{V}_1 &= x_1^T \dot{x}_1 = x_1^T E\tilde{\omega} = x_1^T \left(x_2 + \tilde{\omega}_{p,1}\right) \\ &= -k_1 x_1^T \frac{x_1}{\sqrt{\|x_1\|^2 + \sigma^2}} - k_2 x_1^T x_1 + x_1^T x_2. \end{aligned} \tag{23}$$

Using Lemma 7, the following equation is derived:

$$\begin{aligned} \dot{V}_1 &= -k_1 x_1^T \frac{x_1}{\sqrt{\|x_1\|^2 + \sigma^2}} - k_2 x_1^T x_1 + x_1^T x_2 \\ &\leq -k_1 \|x_1\| - \left(k_2 - \frac{1}{2}\right) \|x_1\|^2 + \frac{\|x_2\|^2}{2} + k_1 \sigma. \end{aligned} \tag{24}$$

Step 2. With Remark 2 and the result in Equation (24), consider the Lyapunov function as follows:

$$V_2^* = V_1 + \frac{1}{2} x_2^T J x_2. \tag{25}$$

Then, the derivative of V_2^* can be calculated as follows:

$$\begin{aligned} \dot{V}_2^* &= \dot{V}_1 + x_2^T J \dot{x}_2 = -k_1 \|x_1\| - \left(k_2 - \frac{1}{2}\right) \|x_1\|^2 + \frac{\|x_2\|^2}{2} \\ &\quad + k_1 \sigma + x_2^T J \dot{E} \tilde{\omega} + x_2^T E \Big[-\left(\tilde{\omega} + \tilde{R}^T \omega_d\right)^\times J \left(\tilde{\omega} + \tilde{R}^T \omega_d\right) \\ &\quad - J \tilde{R}^T \dot{\omega}_d + J \tilde{\omega}^\times \tilde{R}^T \omega_d + d + u - E^{-1} J \dot{\tilde{\omega}}_{p,1} \Big]. \end{aligned} \tag{26}$$

The notation is selected as follows:

$$\begin{aligned} H &= J\dot{E}\tilde{\omega} - J\dot{\tilde{\omega}}_{p,1} + E\Big(-\left(\tilde{\omega} + \tilde{R}^T \omega_d\right)^\times J \left(\tilde{\omega} + \tilde{R}^T \omega_d\right) \\ &\quad - J \tilde{R}^T \dot{\omega}_d + J \tilde{\omega}^\times \tilde{R}^T \omega_d \Big). \end{aligned} \tag{27}$$

From Assumption 1 and Lemma 4, the term $x_2^T E d$ is known to satisfy the following condition:

$$\left\| x_2^T E d \right\| \leq \frac{D}{2} \|x_2\|. \tag{28}$$

Thus, Equation (27) is rewritten as follows:

$$\begin{aligned} \dot{V}_2^* &\leq -\sqrt{2} k_1 V_1^{1/2} - (2k_2 - 1) V_1 + \frac{\|x_2\|^2}{2} + k_1 \sigma + x_2^T H \\ &\quad + \frac{D}{2} \|x_2\| + x_2^T E u. \end{aligned} \tag{29}$$

Observing Lemma 3, H can be expressed as follows:

$$H = W^{*T} h + \varepsilon, \tag{30}$$

where $W^* = [W_1{}^*, W_2{}^*, W_3{}^*]^T$ is a Ge-Lee matrix defining the weight matrix, $h = [h_1, h_2, h_3]^T$ is a Ge-Lee matrix defining the radial basis function matrix, and ε is the approximation error satisfying $\|\varepsilon\| \leq \varepsilon_d$ with $\varepsilon_d > 0$. $W_i{}^*$, $i = 1, 2, 3$, and h_i are three-dimensional Ge-Lee vectors. Combining Equations (29)–(31) results in

$$\begin{aligned} \dot{V}_2^* &\leq -\sqrt{2} k_1 V_1^{1/2} - (2k_2 - 1) V_1 + \frac{\|x_2\|^2}{2} + k_1 \sigma \\ &\quad + x_2^T \left(W^{*T} h + \varepsilon\right) + \frac{D}{2} \|x_2\| + x_2^T E u. \end{aligned} \tag{31}$$

Here, the term $x_2^T W^{*T} h$ can be defined as follows:

$$x_2^T W^* h = \sum_{i=1}^{3} x_{2i} W_i{}^{*T} h_i. \tag{32}$$

Equation (31) is further equivalent to the following:

$$\begin{aligned} \dot{V}_2^* &\leq -\sqrt{2} k_1 V_1^{1/2} - (2k_2 - 1) V_1 + \frac{\|x_2\|^2}{2} + k_1 \sigma \\ &\quad + \sum_{i=1}^{3} \frac{\beta x_{2i}^2 \|h_i\|^2}{2\eta} + \frac{3\eta}{2} + \|x_2\| \left(\frac{D}{2} + \varepsilon_d\right) + x_2^T E u, \end{aligned} \tag{33}$$

where $\beta = \max_{1 \leq i \leq 3} \{\|W_i{}^*\|^2\}$ and η is a positive constant. Thus, β is easier to estimate than W^*. To simplify the design, we introduce a constant $\widehat{D}$ satisfying $\widehat{D} = (D/2) + \varepsilon_d$.

Step 3. In the healthy condition of the actuator, $\delta_i = 1$ is ensured. However, in practical applications, external disturbance and actuator faults always occur simultaneously. Thus, the design of a fault-tolerant controller is necessary.

The fault-tolerant control scheme is designed as follows:

$$u = E^{-1}(u_1 + u_2), \tag{34}$$

$$u_1 = -k_3 x_2 - k_4 \mathrm{sig}(x_2)^\lambda - \widehat{\beta}\frac{x_3 \circ (h \circ h)}{2\eta} - \widehat{D}\tanh\left(\frac{x_2}{\mu_1}\right), \tag{35}$$

$$u_2 = -\widehat{\gamma}\|u_1\|\tanh\left(\frac{x_2\|u_1\|}{\mu_2}\right), \tag{36}$$

$$\dot{\widehat{\beta}} = c_1\left(\sum_{i=1}^{3}\frac{x_{2i}^2\|h_i\|^2}{2\eta} - c_4\widehat{\beta}\right), \tag{37}$$

$$\dot{\widehat{\gamma}} = c_2\left(\|u_1\|\|x_2\|\tanh\left(\frac{\|u_1\|\|x_2\|}{3\mu_2}\right) - c_5\widehat{\gamma}\right), \tag{38}$$

$$\dot{\widehat{D}} = c_3\left(\|x_2\|\tanh\left(\frac{\|x_2\|}{3\mu_1}\right) - c_6\widehat{D}\right), \tag{39}$$

where $\widehat{\beta}$, $\widehat{D}$, and $\widehat{\gamma}$ are estimations of β, D, and γ, respectively, with $\gamma = (1-\theta)/\theta$, $k_3 > 1/2$, $k_4 > 0$, $\mu_1 > 0$, $\mu_2 > 0$, and $c_i > 0$, $i = 1, 2, \cdots, 6$.

Remark 8. Inertial parameters are totally unknown to designers in this paper. To deal with the unmodeled dynamics, the MLP method is adopted to ensure finite-time convergence for the spacecraft system. In Equation (35), the term $k_3x_2 + k_4\mathrm{sig}(x_2)^\lambda$ is introduced for finite-time convergence while $(\widehat{\beta}x_2 \circ (h \circ h))/2\eta$ and $\widehat{D}\tanh(x_2/\mu_1)$ are designed to estimate unknown dynamics and the upper bound of external disturbances.

Remark 9. When $0 < \delta_i < 1$ holds, the spacecraft encounters the partial actuator effectiveness loss fault, which will cause considerable performance degradation. To this end, the fault-tolerant controller is proposed as Equation (34). Here, u_1 implies the norm part of this controller dedicating to forcing spacecraft towards the desired attitude. u_2 defines the compensation part for the actuator fault. With this control strategy, finite-time stability is achievable for tracking errors even when actuator faults occur.

Theorem 10. *For the attitude error dynamics expressed in Equations (10), (11), (19), and (20) with Assumption 1, then, the virtual angular velocity $\tilde{\omega}_{p,1}$ is derived as Equation (21). If the virtual control law and actual control law are designed as in Equations (21) and (34)–(39), the following conclusions can be obtained:*

(i) The region of attraction is represented as follows:

$$x_1^T(0)x_1(0) + x_2^T(0)Jx_2(0) + \frac{1}{c_1}\tilde{\beta}^2(0) + \frac{\theta}{c_2}\tilde{\gamma}^2(0) + \frac{1}{c_3}\tilde{D}^2(0) < 1. \tag{40}$$

(ii) x_2 will be stabilized in the region $\max\{\sqrt{2/(\lambda_{\min}(J))}(\Delta_4/\rho_4), \sqrt{2/(\lambda_{\min}(J))}(\Delta_4/\rho_4)^{1/(\lambda+1)}\}$ *within a finite time. Here,* $\rho_4 = \min\{\sqrt{2}k_1, k_4(2/(\lambda_{\min}(J)))^{(1+\lambda)/2}, ((c_4c_1(2k_5-1))/k_5)^{1/2}, ((c_5c_2(2k_6-1))/\theta k_6)^{1/2}, ((c_6c_3(2k_7-1))/k_7)^{1/2}\}$ *and* $\Delta_4 = (c_4k_5/2)\beta^2 + (c_6k_7/2)\widehat{D}^2 + (c_5k_6/2)\gamma^2 + 3\kappa(D\mu_1 + \mu_2\gamma\theta) + k_1\sigma + (3\eta/2)$. *$k_i$, $i = 5, 6, 7$, are positive constants satisfying $k_i > 0.5$*

Proof. The Lyapunov function can be established as follows:

$$V_3 = V_2^* + \frac{1}{2c_1}\tilde{\beta}^2 + \frac{\theta}{2c_2}\tilde{\gamma}^2 + \frac{1}{2c_3}\tilde{D}^2. \tag{41}$$

Considering Equations (33) and (34), the derivation can be calculated as follows:

$$\begin{aligned}\dot{V}_3 &= \dot{V}_2^* + \frac{1}{c_1}\tilde{\beta}\dot{\tilde{\beta}} + \frac{\theta}{c_2}\tilde{\gamma}\dot{\tilde{\gamma}} + \frac{1}{c_3}\tilde{D}\dot{\tilde{D}} \le -\sqrt{2}k_1V_1^{1/2} \\ &\quad - (2k_2-1)V_1 + \frac{\|x_2\|^2}{2} + k_1\sigma + \sum_{i=1}^{3}\frac{\beta x_{2i}^2\|h_i\|^2}{2\eta} \\ &\quad + \frac{3\eta}{2} + x_2^T(I-\delta)u_1 + x_2^Tu_1 + x_2^T\delta u_2 + \|x_2\|\left(\frac{D}{2}+\varepsilon\right) \\ &\quad - \frac{1}{c_1}\tilde{\beta}\dot{\widehat{\beta}} - \frac{\theta}{c_2}\tilde{\gamma}\dot{\widehat{\gamma}} - \frac{1}{c_3}\tilde{D}\dot{\widehat{D}}.\end{aligned} \tag{42}$$

Then, learning from Equations (35) and (36), one has

$$\begin{aligned}\dot{V}_3 &\le -(2k_2-1)V_1 + \frac{\|x_2\|^2}{2} + k_1\sigma + \sum_{i=1}^{3}\frac{\beta x_{2i}^2\|h_i\|^2}{2\eta} + \frac{3\eta}{2} \\ &\quad + x_2^T(I-\delta)u_1 - k_3\|x_2\|^2 - k_4\|x_2\|^{1+\lambda} - x_2^T\widehat{\beta}\frac{x_2 \circ (h\circ h)}{2\eta} \\ &\quad - \widehat{D}x_2^T\tanh\left(\frac{x_2}{\mu_1}\right) - \widehat{\gamma}\theta x_2^T\|u_1\|\tanh\left(\frac{x_2\|u_1\|}{\mu_2}\right) \\ &\quad + \widehat{D}\|x_2\| - \frac{1}{c_1}\tilde{\beta}\dot{\widehat{\beta}} - \frac{\theta}{c_2}\tilde{\gamma}\dot{\widehat{\gamma}} - \frac{1}{c_3}\tilde{D}\dot{\widehat{D}} \le -(2k_2-1)V_1 \\ &\quad - \left(k_3 - \frac{1}{2}\right)\|x_2\|^2 + k_1\sigma + \sum_{i=1}^{3}\frac{\tilde{\beta}x_{2i}^2\|h_i\|^2}{2\eta} + \frac{3\eta}{2} \\ &\quad + (1-\theta)\|x_2\|\|u_1\| - \widehat{D}\|x_2\| + 3\widehat{D}\mu_1\kappa - \widehat{\gamma}\theta\|x_2\|\|u_1\| \\ &\quad + 3\mu_2\widehat{\gamma}\theta\kappa + \widehat{D}\|x_2\| - \frac{1}{c_1}\tilde{\beta}\dot{\widehat{\beta}} - \frac{\theta}{c_2}\tilde{\gamma}\dot{\widehat{\gamma}} - \frac{1}{c_3}\tilde{D}\dot{\widehat{D}} \\ &= -(2k_2-1)V_1 - \left(k_3 - \frac{1}{2}\right)\|x_2\|^2 + \sum_{i=1}^{3}\frac{\tilde{\beta}x_{2i}^2\|h_i\|^2}{2\eta} \\ &\quad + \theta\tilde{\gamma}\|x_2\|\|u_1\| + \tilde{D}\|x_2\| - \frac{1}{c_1}\tilde{\beta}\dot{\widehat{\beta}} - \frac{\theta}{c_2}\tilde{\gamma}\dot{\widehat{\gamma}} - \frac{1}{c_3}\tilde{D}\dot{\widehat{D}} \\ &\quad + 3\kappa\left(\widehat{D}\mu_1 + \mu_2\widehat{\gamma}\theta\right) + k_1\sigma + \frac{3\eta}{2}.\end{aligned} \tag{43}$$

Combining adaptive laws in Equations (37)–(39), one can obtain the following result:

$$\begin{aligned}
\dot{V}_3 \le& -(2k_2-1)V_1-\left(k_3-\frac{1}{2}\right)\|x_2\|^2+\sum_{i=1}^{3}\frac{\tilde{\beta}x_{2i}^2\|h_i\|^2}{2\eta}\\
&+\theta\tilde{\gamma}\|x_2\|\|u_1\|+\tilde{D}\|x_2\|-\tilde{\beta}\left(\sum_{i=1}^{3}\frac{x_{2i}^2\|h_i\|^2}{2\eta}-c_4\widehat{\beta}\right)\\
&-\theta\tilde{\gamma}\left(\|u_1\|\|x_2\|\tanh\left(\frac{\|u_1\|\|x_2\|}{3\mu_2}\right)-c_5\widehat{\gamma}\right)\\
&-\tilde{D}\left(\|x_2\|\tanh\left(\frac{\|x_2\|}{3\mu_1}\right)-c_6\widehat{D}\right)+3\kappa\left(\widehat{D}\mu_1+\mu_2\widehat{\gamma}\theta\right)\\
&+k_1\sigma+\frac{3\eta}{2}\le-(2k_2-1)V_1-\left(k_3-\frac{1}{2}\right)\|x_2\|^2+c_4\tilde{\beta}\widehat{\beta}\\
&+3\kappa\mu_2\tilde{\gamma}\theta+c_5\theta\tilde{\gamma}\widehat{\gamma}+3\kappa\mu_1\tilde{D}+c_6\tilde{D}\widehat{D}+3\kappa\left(\widehat{D}\mu_1+\mu_2\widehat{\gamma}\theta\right)\\
&+k_1\sigma+\frac{3\eta}{2}\le-(2k_2-1)V_1-\left(k_3-\frac{1}{2}\right)\|x_2\|^2-\frac{c_4}{2}\tilde{\beta}^2\\
&-\frac{c_5\theta}{2}\tilde{\gamma}^2-\frac{c_6}{2}\tilde{D}^2+\frac{c_4}{2}\beta^2+\frac{c_5\theta}{2}\gamma^2+\frac{c_6}{2}D^2\\
&+3\kappa(D\mu_1+\mu_2\gamma\theta)+k_1\sigma+\frac{3\eta}{2}\le-\rho_3V_3+\Delta_3,
\end{aligned}\tag{44}$$

where $\rho_3=\min\{2k_2-1,(2k_3-1)/(\lambda_{\max}(J)),c_1c_4,c_2c_5,c_3c_6\}$ and $\Delta_3=(c_4/2)\beta^2+(c_6/2)D^2+(c_5\theta/2)\gamma^2+k_1\sigma+(3\eta/2)3\kappa(D\mu_1+\mu_2\gamma\theta)$.

Consequently, V_3 is asymptotically stable and converges to a region containing the origin. To proceed, the derivation of V_3 in Equation (42) can be rewritten as follows:

$$\begin{aligned}
\dot{V}_4 \le& -\sqrt{2}k_1V_1^{1/2}+\frac{\|x_2\|^2}{2}+k_1\sigma+\sum_{i=1}^{3}\frac{\beta x_{2i}^2\|h_i\|^2}{2\eta}+\frac{3\eta}{2}\\
&+x_2^T(I-\delta)u_1+x_2^Tu_1+x_2^T\delta u_2+\|x_2\|\left(\frac{D}{2}+\varepsilon\right)\\
&-\frac{1}{c_1}\tilde{\beta}\dot{\widehat{\beta}}-\frac{1}{c_3}\tilde{D}\dot{\widehat{D}}-\frac{\theta}{c_2}\tilde{\gamma}\dot{\widehat{\gamma}}.
\end{aligned}\tag{45}$$

Combining the control laws Equations (34)–(39), the following expression is obtained:

$$\begin{aligned}
\dot{V}_4 \le& -\sqrt{2}k_1V_1^{1/2}-k_4\|x_2\|^{1+\lambda}+c_4\tilde{\beta}\widehat{\beta}+c_5\theta\tilde{\gamma}\widehat{\gamma}+c_6\tilde{D}\widehat{D}\\
&+3\kappa(D\mu_1+\mu_2\gamma\theta)+k_1\sigma+\frac{3\eta}{2}=-\sqrt{2}k_1\left(\frac{1}{2}x_1^Tx_1\right)^{1/2}\\
&-k_4\left(\frac{2}{\lambda_{\min}(J)}\right)^{(1+\lambda)/2}\left(\frac{1}{2}x_2^TJx_2\right)^{(1+\lambda)/2}+c_4\tilde{\beta}\widehat{\beta}+c_5\theta\tilde{\gamma}\widehat{\gamma}\\
&+c_6\tilde{D}\widehat{D}+3\kappa(D\mu_1+\mu_2\gamma\theta)+k_1\sigma+\frac{3\eta}{2}.
\end{aligned}\tag{46}$$

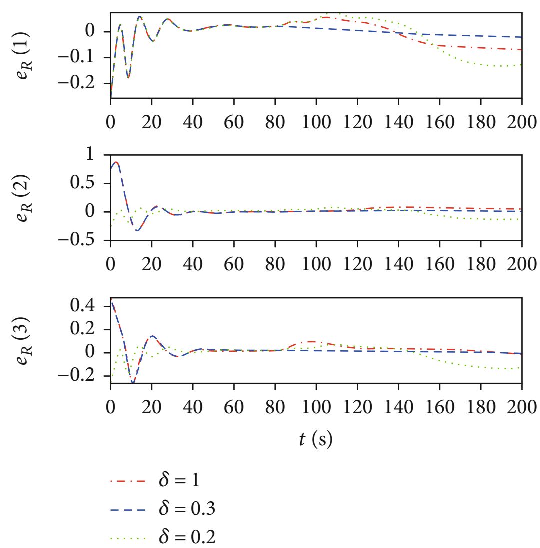

Figure 1: Attitude tracking errors under different δ.

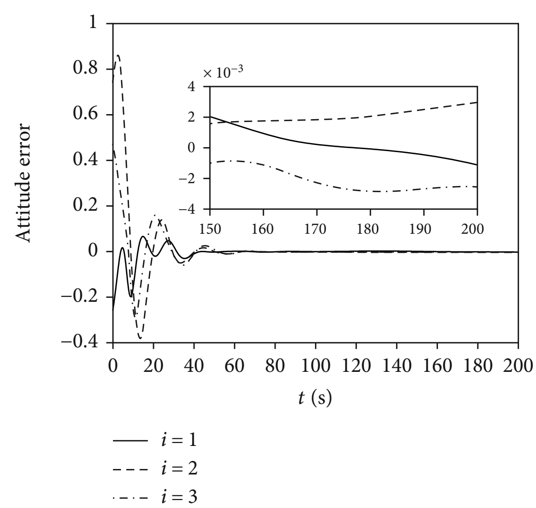

Figure 2: Attitude tracking error using the finite-time controller.

For the term $c_4\tilde{\beta}\widehat{\beta}$, the following condition always exists:

$$\begin{aligned}
c_4\tilde{\beta}\widehat{\beta}=c_4\left(-\tilde{\beta}^2+\tilde{\beta}\beta\right)\le c_4\left(-\tilde{\beta}^2+\frac{1}{2k_5}\tilde{\beta}^2+\frac{k_5}{2}\beta^2\right)\\
\le\frac{-c_4(2k_5-1)}{2k_5}\tilde{\beta}^2+\frac{c_4k_5}{2}\beta^2,
\end{aligned}\tag{47}$$

where k_5 is a positive constant. If it satisfies $((c_4(2k_5-1))/2k_5)\tilde{\beta}^2\ge1$, the following equation is obtained:

$$\left(\frac{c_4(2k_5-1)}{2k_5}\tilde{\beta}^2\right)^{1/2}+c_4\tilde{\beta}\widehat{\beta}\le\frac{c_4(2k_5-1)}{2k_5}\tilde{\beta}^2+c_4\tilde{\beta}\widehat{\beta}\le\frac{c_4k_5}{2}\beta^2.\tag{48}$$

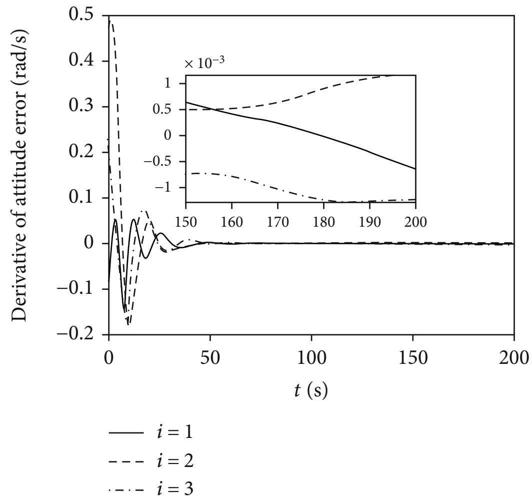

Figure 3: Derivative of $e_{\tilde{R}}$ using the finite-time controller.

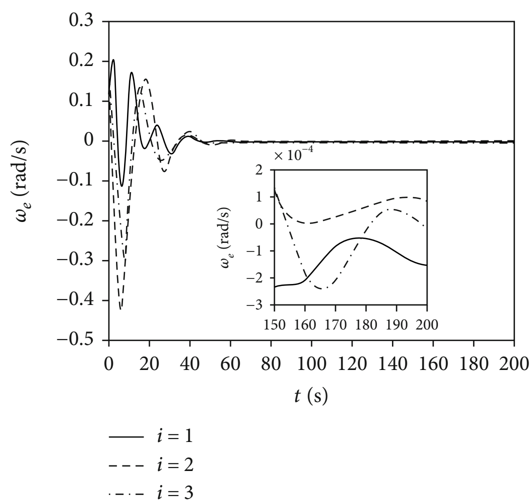

Figure 4: Angular velocity tracking error using the finite-time controller.

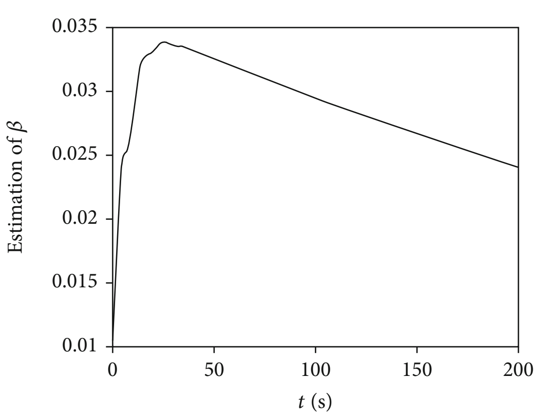

Figure 5: Estimation of β.

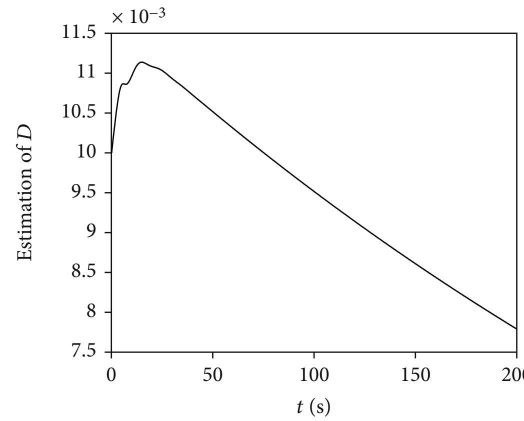

Figure 6: Estimation of $\widehat{D}$.

If $((c_4(2k_5-1))/2k_5)\tilde{\beta}^2 < 1$ exists, the following equation is obtained:

$$\left(\frac{c_4(2k_5-1)}{2k_5}\tilde{\beta}^2\right)^{1/2}\Bigg|_{((c_4(2k_5-1))/2k_5)\tilde{\beta}^2<1} < \left(\frac{c_4(2k_5-1)}{2k_5}\tilde{\beta}^2\right)^{1/2}\Bigg|_{((c_4(2k_5-1))/2k_5)\tilde{\beta}^2\geq 1}. \quad (49)$$

Then, it follows

$$\left(\frac{c_4(2k_5-1)}{2k_5}\tilde{\beta}^2\right)^{1/2} + c_4\tilde{\beta}\widehat{\beta} \leq \frac{c_4 k_5}{2}\beta^2. \quad (50)$$

The same results for $c_5\theta\tilde{\gamma}\widehat{\gamma}$ and $c_6\tilde{D}\widehat{D}$ are obtained. Consequently, Equation (46) can be rewritten as follows:

$$\begin{aligned}
\dot{V}_4 \leq & -\sqrt{2}k_1\left(\frac{1}{2}x_1^T x_1\right)^{1/2} - k_4\left(\frac{2}{\lambda_{\min}(J)}\right)^{(1+\lambda)/2}\left(\frac{1}{2}x_2^T J x_2\right)^{(1+\lambda)/2} \\
& -\left(\frac{c_4 c_1(2k_5-1)}{k_5}\right)^{1/2}\left(\frac{1}{2c_1}\tilde{\beta}^2\right)^{1/2} - \left(\frac{c_5 c_2(2k_6-1)}{\theta k_6}\right)^{1/2}\left(\frac{\theta}{2c_2}\tilde{\gamma}^2\right)^{1/2} \\
& -\left(\frac{c_6 c_3(2k_7-1)}{k_7}\right)^{1/2}\left(\frac{1}{2c_3}\tilde{D}^2\right)^{1/2} + \left(\frac{c_4(2k_5-1)}{2k_5}\tilde{\beta}^2\right)^{1/2} \\
& +\left(\frac{c_5(2k_6-1)}{2k_6}\tilde{\gamma}^2\right)^{1/2} + \left(\frac{c_6(2k_7-1)}{2k_7}\tilde{D}^2\right)^{1/2} + c_4\tilde{\beta}\widehat{\beta} \\
& + c_5\theta\tilde{\gamma}\widehat{\gamma} + c_6\tilde{D}\widehat{D} + 3\kappa(D\mu_1 + \mu_2\gamma\theta) + k_1\sigma + \frac{3\eta}{2} \\
\leq & -\rho_4 \min\left\{V_4^{1/2}, V_4^{(1+\lambda)/2}\right\} + \left(\frac{c_4(2k_5-1)}{2k_5}\tilde{\beta}^2\right)^{1/2} \\
& +\left(\frac{c_5(2k_6-1)}{2k_6}\tilde{\gamma}^2\right)^{1/2} + \left(\frac{c_6(2k_7-1)}{2k_7}\tilde{D}^2\right)^{1/2} + c_4\tilde{\beta}\widehat{\beta} \\
& + c_5\theta\tilde{\gamma}\widehat{\gamma} + c_6\tilde{D}\widehat{D} + 3\kappa(D\mu_1 + \mu_2\gamma\theta) + k_1\sigma + \frac{3\eta}{2}.
\end{aligned} \quad (51)$$

In terms of Equation (50), we have

$$\begin{aligned}\dot{V}_4 &\le -\rho_4 \min\left\{V_4^{1/2}, V_4^{(1+\lambda)/2}\right\} + \frac{c_4 k_5}{2}\beta^2 + \frac{c_6 k_7}{2}\widehat{D}^2 + \frac{c_5 k_6}{2}\gamma^2 \\ &\quad + 3\kappa(D\mu_1 + \mu_2\gamma\theta) + k_1\sigma + \frac{3\eta}{2} \\ &= -\rho_4 \min\left\{V_4^{1/2}, V_4^{(1+\lambda)/2}\right\} + \Delta_4. \end{aligned} \tag{52}$$

From Equation (52), it can be concluded that the result $\dot{V}_4 \le 0$ always holds. Consequently, x_1, x_2, $\tilde{\beta}$, $\tilde{\gamma}$, and $\tilde{D}$ are all bounded. To keep $\|x_1\|^2 < 1$, one can obtain

$$\begin{aligned} V_4 \le V_4(0) &\le \frac{1}{2}x_1^T(0)x_1(0) + \frac{1}{2}x_2^T(0)Jx_2(0) + \frac{1}{2c_1}\tilde{\beta}^2(0) \\ &\quad + \frac{1}{2c_2}\tilde{D}^2(0) < \frac{1}{2}. \end{aligned} \tag{53}$$

Therefore, (i) has been proved.

Meanwhile, according to Lemma 6, x_2 will be stabilized to the region $\max\{\sqrt{2/(\lambda_{\min}(J))}(\Delta_4/\rho_4), \sqrt{2/(\lambda_{\min}(J))}(\Delta_4/\rho_4)^{1/(\lambda+1)}\}$ within a finite time.

Thus, Theorem 10 is proven.

4. Simulation Results

This section is dedicated to authenticating the stability and validity of the controllers presented in the theoretical analysis. The main parameters, inertial matrix, disturbance torque, initial state, desired rotation matrix, and angular velocity are selected as follows: $J = \begin{bmatrix} 22.7 & 0 & 0 \\ 0 & 23.3 & 0 \\ 0 & 0 & 24.5 \end{bmatrix}$ kg · m², $R(0) = \begin{bmatrix} 0.4977 & -0.8674 & -0.0007 \\ 0 & -0.0008 & 1.0000 \\ -0.8674 & -0.4977 & -0.0004 \end{bmatrix}$, $\omega(0) = [0.1, 0.1, 0.1]^T$ rad/s, $R_d(0) = I_{3\times3}$, $\omega_d = 0.1 \times [\sin(t/40), -\cos(t/50), -\sin(t/60)]^T$ rad/s, and $d = 0.02 \times [\sin(0.1t), \cos(0.2t), \sin(0.2t)]^T$, respectively.

To show the adverse effect of the actuator faults, the control performance of the controller in [22] is shown under two scenarios $\delta = \begin{cases} \text{diag}(0.3, 0.3, 0.3), & \text{if } t > 80\text{s} \\ \text{diag}(1, 1, 1), & \text{else} \end{cases}$ and $\delta = \begin{cases} \text{diag}(0.2, 0.2, 0.2), & \text{if } t > 80\text{s} \\ \text{diag}(1, 1, 1), & \text{else} \end{cases}$, where $d = 0.05 \times [\sin(0.1t), \cos(0.2t), \sin(0.2t)]^T$ N · m. Attitude tracking errors are presented in Figure 1, which implies that system performance degradation will be caused as δ increases. Thus, it concludes that fault-tolerant control strategies are necessary for spacecraft during space missions in case of actuator faults.

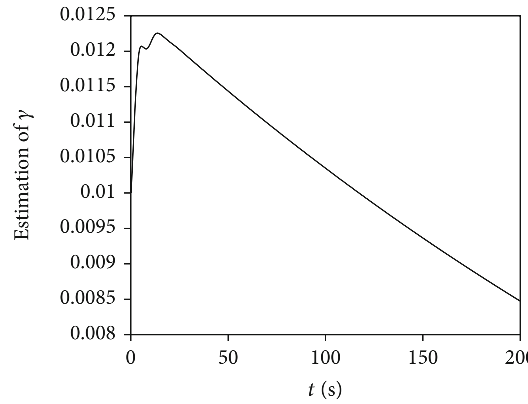

Figure 7: Estimation of γ.

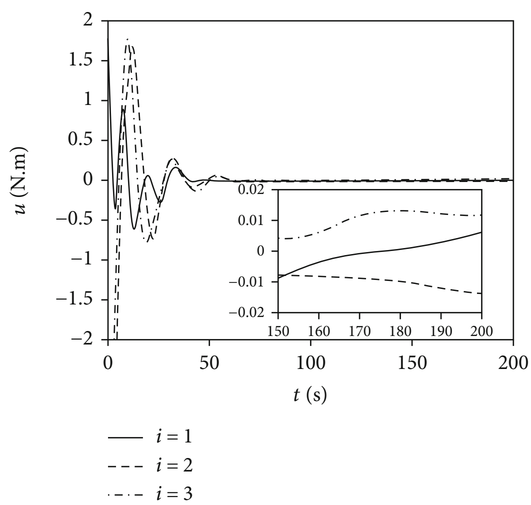

Figure 8: Control torque using the finite-time controller.

Then, the actuator faults are set as follows: $\delta = \begin{cases} \text{diag}(0.5, 0.4, 0.3), & \text{if } t > 100\text{s} \\ \text{diag}(1, 1, 1), & \text{else} \end{cases}$. The design parameters of the fault-tolerant controller are determined as follows: $k_1 = 0.05$, $k_2 = 0.5$, $k_3 = 2$, $k_4 = 1$, $c_1 = 0.001$, $c_2 = 0.001$, $c_3 = 0.001$, $c_4 = 2$,, $c_5 = 2$, $c_6 = 2$, $\mu_1 = 1$, $\mu_2 = 1$, and $\lambda = 0.9$. The following parameters are selected for the RBF NN: $b_i = 2$, $p = 20$, and the input vectors of the RBF NN satisfy $\omega_i \in [-0.5, 0.5]$rad/s, $\dot{\omega}_i \in [-0.5, 0.5]$rad/s, $x_{1i} \in [-0.3, 0.3]$, $x_{2i} \in [-0.5, 0.5]$rad/s, and $x_{2di} \in [-0.5, 0.5]$rad/s. Simulation results for this method are presented in Figures 2–8. From the simulation results, we can conclude that the control objective can be achieved within 60 s in the case of actuator faults. Additionally, the chattering problem does not appear in the control torque. Thus, the points mentioned in Theorem 10 are illustrated by the simulation results.

5. Conclusions

In this paper, the unwinding-free problem is solved for spacecraft attitude tracking control missions. The proposed control schemes not only exhibit excellent robustness against actuator faults and disturbance but also address the unknown inertial parameters. Additionally, the application of the MLP method results in a controller with less computational complexity. The simulation results prove the effectiveness of the proposed methods.

Data Availability

No data were used to support this study.

Conflicts of Interest

The authors declare that they have no conflicts of interest.

References

[1] L. Zhao, J. Yu, and P. Shi, "Command filtered backstepping-based attitude containment control for spacecraft formation," *IEEE Transactions on Systems, Man, and Cybernetics: Systems*, 2019.

[2] F. Wang, M. Hou, X. Cao, and G. Duan, "Event-triggered backstepping control for attitude stabilization of spacecraft," *Journal of the Franklin Institute*, vol. 356, no. 16, pp. 9474–9501, 2019.

[3] C. Zhang, G. Ma, Y. Sun, and C. Li, "Simple model-free attitude control design for flexible spacecraft with prescribed performance," *Proceedings of the Institution of Mechanical Engineers, Part G: Journal of Aerospace Engineering*, vol. 233, no. 8, pp. 2760–2771, 2019.

[4] Q. Zhao and G. Duan, "Adaptive finite-time tracking control of 6DOF spacecraft motion with inertia parameter identification," *IET Control Theory & Applications*, vol. 13, no. 13, pp. 2075–2085, 2019.

[5] D. Chakrabarti and S. Narayanasamy, "PD and PDβ based sliding mode control algorithms with modified reaching law for satellite attitude maneuver," *Advances in Space Research*, vol. 65, no. 4, pp. 1279–1295, 2019.

[6] J. Qiao, Z. Li, J. Xu, and X. Yu, "Composite nonsingular terminal sliding mode attitude controller for spacecraft with actuator dynamics under matched and mismatched disturbances," *IEEE Transactions on Industrial Informatics*, vol. 16, no. 2, pp. 1153–1162, 2019.

[7] Y. Guo, B. Huang, J. Guo, A. J. Li, and C. Q. Wang, "Velocity-free sliding mode control for spacecraft with input saturation," *Acta Astronautica*, vol. 154, pp. 1–8, 2019.

[8] C. Zhang, G. Ma, Y. Sun, and C. Li, "Observer-based prescribed performance attitude control for flexible spacecraft with actuator saturation," *ISA Transactions*, vol. 89, pp. 84–95, 2019.

[9] Q. Hu, X. Shao, and L. Guo, "Adaptive fault-tolerant attitude tracking control of spacecraft with prescribed performance," *IEEE/ASME Transactions on Mechatronics*, vol. 23, no. 1, pp. 331–341, 2017.

[10] X. Shao, Q. Hu, Y. Shi, and B. Jiang, "Fault-tolerant prescribed performance attitude tracking control for spacecraft under input saturation," *IEEE Transactions on Control Systems Technology*, vol. 28, no. 2, pp. 574–582, 2018.

[11] C. Wang, L. Guo, C. Wen, Q. Hu, and J. Qiao, "Event-triggered adaptive attitude tracking control for spacecraft with unknown actuator faults," *IEEE Transactions on Industrial Electronics*, vol. 67, no. 3, pp. 2241–2250, 2019.

[12] B. Wu, Q. Shen, and X. Cao, "Event-triggered attitude control of spacecraft," *Advances in Space Research*, vol. 61, no. 3, pp. 927–934, 2018.

[13] B. Huang, S. Zhang, Y. He, B. Wang, and Z. Deng, "Finite-time anti-saturation control for Euler–Lagrange systems with actuator failures," *ISA Transactions*, 2020.

[14] B. Liu, M. Hou, C. Wu, W. Wang, Z. Wu, and B. Huang, "Predefined-time backstepping control for a nonlinear strict-feedback system," *International Journal of Robust and Nonlinear Control*, 2021.

[15] Y. Guo, S. M. Song, and X. H. Li, "Finite-time output feedback attitude coordination control for formation flying spacecraft without unwinding," *Acta Astronautica*, vol. 122, pp. 159–174, 2016.

[16] Y. Guo, J. Guo, and S. Song, "Backstepping control for attitude tracking of the spacecraft under input saturation," *Acta Astronautica*, vol. 138, pp. 318–325, 2017.

[17] Y. Guo, S. M. Song, X. H. Li, and P. Li, "Terminal sliding mode control for attitude tracking of spacecraft under input saturation," *Journal of Aerospace Engineering*, vol. 30, no. 3, article 06016006, 2017.

[18] Y. Guo, B. Huang, S. Song, A. J. Li, and C. Q. Wang, "Robust saturated finite-time attitude control for spacecraft using integral sliding mode," *Journal of Guidance, Control, and Dynamics*, vol. 42, no. 2, pp. 440–446, 2019.

[19] Z. Yin, A. Suleman, J. Luo, and C. Wei, "Appointed-time prescribed performance attitude tracking control via double performance functions," *Aerospace Science and Technology*, vol. 93, p. 105337, 2019.

[20] M. Liu, X. Shao, and G. Ma, "Appointed-time fault-tolerant attitude tracking control of spacecraft with double-level guaranteed performance bounds," *Aerospace Science and Technology*, vol. 92, pp. 337–346, 2019.

[21] B. Huang, B. Zhou, S. Zhang, and C. Zhu, "Adaptive prescribed performance tracking control for underactuated autonomous underwater vehicles with input quantization," *Ocean Engineering*, vol. 221, p. 108549, 2021.

[22] X. Wu, H. Zhao, B. Huang, J. Li, S. Song, and R. Liu, "Minimum-learning-parameter-based anti-unwinding attitude tracking control for spacecraft with unknown inertia parameters," *Acta Astronautica*, vol. 179, pp. 498–508, 2021.

[23] X. Cao, P. Shi, Z. Li, and M. Liu, "Neural-network-based adaptive backstepping control with application to spacecraft attitude regulation," *IEEE transactions on neural networks and learning systems*, vol. 29, no. 9, pp. 4303–4313, 2018.

[24] N. Zhou, R. Chen, Y. Xia, J. Huang, and G. Wen, "Neural network–based reconfiguration control for spacecraft formation in obstacle environments," *International Journal of Robust and Nonlinear Control*, vol. 28, no. 6, pp. 2442–2456, 2018.

[25] S. Mirzajani, M. P. Aghababa, and A. Heydari, "Adaptive control of nonlinear fractional-order systems using T-S fuzzy method," *International Journal of Machine Learning and Cybernetics*, vol. 10, no. 3, pp. 527–540, 2019.

[26] Z. Zhu and Y. Guo, "Adaptive fault-tolerant attitude tracking control for spacecraft formation with unknown inertia,"

International Journal of Adaptive Control and Signal Processing, vol. 32, no. 1, pp. 13–26, 2018.

[27] G. Niu, Q. Hu, and L. Guo, "Iterative disturbance observer design for spacecraft fault-tolerant control with actuator failure," in *2017 36th Chinese Control Conference (CCC)*, Dalian, 2017.

[28] N. Zhou and Y. Xia, "Distributed fault-tolerant control design for spacecraft finite-time attitude synchronization," *International Journal of Robust and Nonlinear Control*, vol. 26, no. 14, pp. 2994–3017, 2016.

[29] B. Hashtarkhani and M. J. Khosrowjerdi, "Neural adaptive fault tolerant control of nonlinear fractional order systems via terminal sliding mode approach," *Journal of Computational & Nonlinear Dynamics*, vol. 14, 2018.

[30] J. H. Bi and K. M. Javad, "Adaptive actuator failure compensation for uncertain nonlinear fractional order strict feedback form systems," *Transactions of the Institute of Measurement and Control*, vol. 41, article 014233121877874, 2018.

[31] B. Huang, A. Li, Y. Guo, and C. Q. Wang, "Rotation matrix based finite-time attitude synchronization control for spacecraft with external disturbances," *ISA Transactions*, vol. 85, pp. 141–150, 2019.

[32] B. Huang, A. Li, Y. Guo, and C. Q. Wang, "Fixed-time attitude tracking control for spacecraft without unwinding," *Acta Astronautica*, vol. 151, pp. 818–827, 2018.

[33] B. Huang, A. Li, Y. Guo, C. Q. Wang, and J. H. Guo, "Finite-time fault-tolerant attitude tracking control for spacecraft without unwinding," *Proceedings of the Institution of Mechanical Engineers, Part G: Journal of Aerospace Engineering*, vol. 233, no. 6, pp. 2119–2130, 2019.

[34] H. U. Qinglei, X. I. Li, and W. A. Chenliang, "Adaptive fault-tolerant attitude tracking control for spacecraft with time-varying inertia uncertainties," *Chinese Journal of Aeronautics*, vol. 32, no. 3, pp. 674–687, 2019.

[35] C. Zhu, B. Huang, B. Zhou, Y. Su, and E. Zhang, "Adaptive model-parameter-free fault-tolerant trajectory tracking control for autonomous underwater vehicles," *ISA Transactions*, 2021.